Guiding research in electrochemical CO$_2$ conversion strategies through a systems-level perspective

Emily Nishikawa,[a] Shamiul Islam,[a] Sylvia Sleep,[b] Viola Birss,[c] Joule Bergerson*[a]

[a.] Department of Chemical and Petroleum Engineering, University of Calgary, 2500 University Drive NW, Calgary, Alberta, Canada, T2N 1N4.
[b.] Department of Civil Engineering, University of Calgary, 2500 University Drive NW, Calgary, Alberta, Canada, T2N 1N4.
[c.] Department of Chemistry, University of Calgary, 2500 University Drive NW, Calgary, Alberta, Canada, T2N 1N4.
*Corresponding author at: 2500 University Drive, NW, Calgary, Alberta T2N 1N4, Canada.
E-mail address: jbergers@ucalgary.ca (J. Bergerson).

Contents

S1. Additional information about the systems under study

S1.1. Electrochemical pathway (SOEC-Co and SOEC-AEC-flow)

In the co-electrolysis strategy (SOEC-Co), for the methanation step, methane can be produced by CO or CO_2 reduction.[1] Both types of catalytic methanation were assumed to have the same energy demand of 0.34 kWh/kg CH_4[2,3] (assumption tested in the sensitivity analysis). For methanol production, the secondary unit has an electricity demand of 1.3 kWh/kg methanol.[2,4]

Data for diesel production from syngas was obtained from Okeke et al.[5] and Okeke and Mani.[6] The fuel gas stream leaving the F-T unit is used for electricity generation,[5] which is directed to offset part of the electrolyzer consumption. The heat produced by the F-T unit was considered to be enough to provide heat to the other units[7]. Figure S4 in this ESI presents a diagram of the diesel process. In a Fischer−Tropsch (FT) process, liquid hydrocarbons are produced by reacting syngas (H_2:CO ratio of 2:1) at a pressure of 25 bar and temperature of 230°C.[7]

Purification of the gaseous stream is assumed to be done by pressure swing adsorption[8] with an energy requirement of 0.25 kWh/m³ relative to a biogas upgrading process.[8,9]

Table 1: Inputs for methane, methanol, and diesel production from SOEC-Co.

Intermediate	Item	Value	Unit
Syngas[10]	CO_2	1.4	kg CO_2/kg syngas
	H_2O	1.2	kg H_2O/kg syngas
	PSA separation	0.030	kWh/kg syngas
	Heat	0.32	kWh/kg syngas
	Electricity	7.3	kWh/kg syngas
	O_2 produced	1.5	kg O_2/kg syngas
Methane[2,3,10]	Syngas	2.0	kg syngas/kg methane
	Electricity for extra H_2	5.7	kWh/kg methane
	Methanation	0.34	kWh/kg methane
Methanol[2,4,10]	Syngas	1.0	kg syngas/kg methanol
	Methanol synthesis	1.3	kWh/kg methanol
Diesel[5,6,10]	Syngas	2.1	kg syngas/kg diesel
	Electricity for electrolysis	14	kWh/kg diesel
	Electricity for F-T	0.071	kWh/kg diesel
	PSA separation	0.063	kWh/kg diesel
	Off-gas emissions	0.62	kg CO_2eq/kg diesel
	Gasoline produced	0.52	kg gasoline/kg diesel
	LPG produced	0.10	kg LPG/kg diesel
	Wax produced	0.025	kg wax/kg diesel
	Steam produced	3.5	kg steam/kg diesel
	O_2 produced	3.2	kg O_2/kg diesel

As mentioned in the main text (section 2.1.1), the syngas composition from co-electrolysis had to be adjusted to H_2:CO molar ratio of 3:1 by adding extra H_2. We estimated the inventory for a co-electrolysis that is tuned to produce the syngas with the desired 3:1 ratio. The H_2O input and the O_2 produced were adjusted, and the remaining parameters were kept constant, per mass of syngas. We deemed this a reasonable assumption since the water electrolysis should not influence the utilities demand in a relevant manner.[11] This is merely an estimate, to understand if in this ideal condition, tuning the syngas composition may be beneficial or not.

In the SOEC-Co pathway, a thermochemical unit is needed, which could be classified as hybrid; however, it was classified as an electrochemical pathway because CO_2 is converted in the electrolyzer (and not only H_2O electrolysis, as in the thermochemical pathway). This classification of pathways was adapted from Grim et al[12].

The CO_2-CO-product process in tandem (SOEC-AEC-flow) and the low-temperature electrolysis in MEA (membrane electrode assembly) with an AEM (anion exchange membrane) are strategies recently developed in the low-temperature electrolysis area.[8,13,14] The CO_2-CO-product tandems are explained in the main text.

The low-temperature electrolysis in MEA (membrane electrode assembly) with an AEM (anion exchange membrane) was not further explored in the main text because in past studies,[8,13] this strategy was economically unfeasible and gave higher GHG emissions compared to the tandem strategy even with optimistic assumptions. In this strategy, humidified CO_2 is fed to the electrolyzer in MEA configuration involving an AEM. The higher voltage of the direct CO_2 electrolysis to produce methane and methanol using this strategy (compared to the combined voltage required for CO_2 to CO electrolysis and CO reduction to products) and CO_2 crossover/carbonate formation led to the higher GHG emissions.

S1.2. Hybrid pathway (water electrolysis, SOEC-W and PEMEC-W)

As mentioned in the main text, SOECs and PEMECs were considered for hydrogen production.

Methane can be produced by the Sabatier reaction[2,3] in a fixed bed reactor by reacting CO_2 and H_2 in the presence of catalysts (ruthenium or nickel-based, for example),[15] at a temperature of 180-350°C. The reported CO_2 consumption is 2.8 kg CO_2/kg methane, the demand of H_2 is 0.52 kg H_2/kg methane, and the electricity consumption of methanation is 0.34 kWh/kg methane.[2,3]

H_2 produced by water electrolysis reacts with CO_2 to produce methanol.[2,4] For methanol production, the CO_2 consumption is 1.4 kg CO_2/kg methanol, the H_2 demand is 0.19 kg H_2/kg methanol, and electricity demand is 1.3 kWh/kg methanol.[2,4]

For diesel production, it is necessary to convert CO_2 to CO using the rWGS reaction, which produces CO with selective water removal.[16] Additional H_2 from the electrolyzer is blended with the product of rWGS to produce syngas with H_2:CO molar ratio of 2:1. The

fuel gas stream leaving the F-T unit is used for electricity generation,[5] which is directed to offset part of the electrolyzer consumption. The heat produced by the F-T unit was considered sufficient to heat the other units.[7] Figure S4 presents a more detailed diagram of the diesel process.

The syngas is then processed in a conventional F-T unit.[5] A process similar to that described by Liu et al.[17] is applied, in which the source of CO_2 is specified as DAC. Oxygen is generated as a co-product in all cases. For diesel, additional co-products are generated: gasoline, liquefied petroleum gas (LPG), wax, and steam.

Table 2: Inputs for methane, methanol, and diesel production from SOEC-W and PEMEC-W.

Intermediate	Item	Value	Unit
Methane[2,3]	CO_2	2.8	kg CO_2/kg methane
	Electricity (SOEC-W)	24	kWh/kg methane
	Electricity (PEMEC-W)	29	kWh/kg methane
	O_2 produced	4.2	kg O_2/kg methane
Methanol[2]	CO_2	1.4	kg CO_2/kg methanol
	Electricity (SOEC-W)	10	kWh/kg methanol
	Electricity (PEMEC-W)	12	kWh/kg methanol
	O_2 produced	1.5	kg O_2/kg methanol
Diesel[5,6,17,18]	CO_2	3.1	kg CO_2/kg diesel
	Electricity (SOEC-W)	18	kWh/kg diesel
	Electricity (PEMEC-W)	21	kWh/kg diesel
	Off-gas emissions	0.62	kg CO_2eq/kg diesel
	Gasoline produced	0.52	kg gasoline/kg diesel
	LPG produced	0.10	kg LPG/kg diesel
	Wax produced	0.025	kg wax/kg diesel
	Steam produced	3.5	kg steam/kg diesel
	O_2 produced	3.1	kg O_2/kg diesel

S1.3. Applications
S1.3.1. Polymer production

For polymer production, methane was used to produce polyoxymethylene (POM), and methanol to produce polypropylene (PP).

In the case of POM from methane, we provide additional information as it may not be intuitive. The route for production is shown in Figure S1; we are showing the intermediate products since[19] the technologies themselves were not specified in the source. There are two types of POM (POM-homopolymer and POM-copolymer), both are considered in the source data[2,19,20] and are produced from methane via methanol, which is oxidized to produce formaldehyde. POM-homopolymer is produced from formaldehyde polymerization, while POM-copolymer requires the conversion of formaldehyde to

trioxane, which is then polymerized to POM with a co-monomer. The methane production process may be from CO_2 conversion, or natural gas (considered the incumbent).
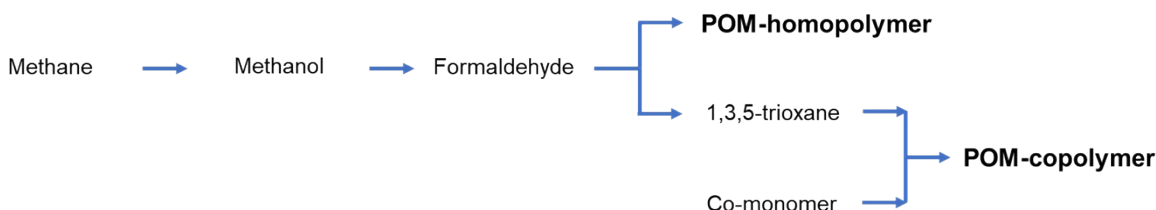

Figure S1: Route for POM production. Adapted from [19]

Table 3: Information for POM and PP production.

Product	Inputs	Unit
POM[2,19,20]	0.35	kg CH_4/kg POM
	6.5	kWh/kg POM
	5	MJ therm/kg POM
PP[2,21]	2.6	kg methanol/kg PP
	3.8	kWh elec/kg PP
	1.6	kWh therm/kg PP
	85	kg cooling water/kg PP
	0.20	kg steam/kg PP

Two alternative end of life treatment were considered for sensitivity analysis: recycling followed by incineration, and direct incineration, both based on Turnau et al.[21] The recycling system consists of four cycles of use and three of recycling. Due to degradation, the virgin material (PP or POM) is sent to incineration after the cycles.

The total electricity demand is 0.49 kWh for recovery and recycling facility in the production of 1.48 kg of useful plastic. The total diesel and tap water demands are 0.018 kg diesel and 0.0014 kg water, respectively. The total amount of plastic incinerated is 1 kg. With recycling, less virgin material (CO_2-based polymers) is required. Therefore, 0.67 kg of virgin polymer is required. The demands of electricity, diesel, water, and polymer sent to incineration were calculated proportionally.

S1.3.2. Transportation

For transportation, Ecoinvent v3.8[22] datasets for a medium-size passenger car complying with Euro 5 standard[23] and fueled by natural gas and diesel[22] were used. Each car was considered to transport, on average, 1.6 passengers.[24] Table S4 presents information for the calculation of transportation process by methane.

Table S4: Information for transportation by methane.

Item	Value	Additional information
Natural gas input[22]	0.077 m³/km	Dataset transport, passenger car, medium size, natural gas, EURO 5
Natural gas density[25]	0.84 kg/m³	
Natural gas heating value[25]	39 MJ/m³	
% of methane in natural gas[26]	82%	
Methane input	0.064 kg CH_4/km	MJ equivalent of natural gas
Output	17 km/kg CH_4	1/0.06 kg CH_4/km
Emissions[22]	0.26 kg CO_2eq/km	

The use per kg of methane was calculated by:

$$17\frac{km}{kg\ CH_4} * 0.26\frac{kg\ CO_2eq}{km} = 4.3\frac{kg\ CO_2eq}{kg\ CH_4}$$

Considering 1.6 passengers, for one passenger (pkm):

$$17\frac{km}{kg\ CH_4} * \frac{1}{1.6} = 10\frac{pkm}{kg\ CH_4}$$

For the functional unit of 1 pkm, each number in kg CO_2eq/kg CH_4 was divided by 10 pkm/kg CH_4 to give emissions in kg CO_2eq/pkm. For methanol and diesel, the same process was applied.

S1.3.3. Power generation

For power generation, Bicer and Khalid[27] study was used for methane and methanol (fuel cell) as feedstock, and Ecoinvent v3.8[22] was used for diesel (heat and power co-generation, 200 kW).

For methane and methanol use, there are two outputs: electricity and heat.[27] Heat displaced emissions are listed in Table S8. Table S5 presents information for the calculation of power generation process by methane.

Table S5: Information for power generation by methane in low carbon scenario.

Item	Value	Additional information
Natural gas input[27]	3.1x10⁵ kg NG/year	
Natural gas density[25]	0.84 kg/m³	
Natural gas heating value	39 MJ/m³	
Methane in natural gas[26]	82%	
Methane input	2.9x10⁵ kg CH_4/year	Equivalent in energy to natural gas
Methane input (for electricity)	1.8x10⁵ kg CH_4/year	Allocation factor applied to CH_4 input to the system
Output[27]	2.0x10³ MWh elec/year	6.8 kWh elec/kg CH_4 4.3 kWh heat/ kg CH_4
Emissions of use	0.40 kg CO_2eq/kWh	The CO_2 emissions come from the

elec	complete methane combustion[28]

For the functional unit of 1 kWh elec, each number in kg CO_2eq/kg CH_4 was divided by 11 kWh elec/kg CH_4 to give emissions in kg CO_2eq/kWh. For methanol and diesel, the same process was applied.

S1.4. Incumbents

The emissions of incumbent processes for polymer production were obtained from Hoppe et al.[2] for PP and from the POM EPD for POM.[19] The conventional production of PP emits 1.9 kg CO_2eq/kg PP, and the conventional production process of POM emits 3.2 kg CO_2eq/kg POM.

For transportation, the incumbent process was considered passenger transportation by medium-size cars fueled by gasoline. The data was obtained from Ecoinvent v3.8 database[22] (dataset transport, passenger car, medium size, petrol, EURO 5). The emissions related to 1 pkm (passenger-kilometer) is 0.21 kg CO_2eq/pkm, considering 1.6 passengers on average.[22]

For electricity, the production from natural gas combined cycle plant was considered the incumbent, with emissions of 0.49 kg CO_2eq/kWh.[29]

The incumbents for the co-products generated in the CCT cases were obtained from the GREET model[30] and Ecoinvent v3.8 database,[22] the emission factors of conventional production processes are listed in the Table S6. Gasoline, LPG, and wax are assumed to be from fossil sources, steam from a natural gas boiler, and oxygen from cryogenic air separation.

Table S6: Emission factors of conventional production processes of co-products. The allocation methods used by the sources, if any, are indicated between parentheses.

Co-product	Emission factor
Gasoline[30]	0.88 kg CO_2eq/kg (Substitution)
LPG[30]	0.58 kg CO_2eq/kg (Substitution)
Steam[30]	0.31 kg CO_2eq/kWh (Substitution)
Wax[22]	0.73 kg CO_2eq/kg (Proxy: paraffin production | paraffin) (Exergy)
O_2[31]	0.20 kWh/kg O_2

The credits were calculated based on the production of each co-product in relation to the production of the main products (methane, methanol, or diesel).

S1.5. Market sizes

For the calculation of the global reduction potential metric, the market sizes of the applications were compiled. Table S7 presents the values considered for calculations.

Market size data by year could not be accessed, and the most recent reported numbers were used.

Table S7: Market sizes of the applications considered in this study.

Application	Market Size	Year
Electricity[32]	2.6×10^4 TWh	2017
Passenger transportation[33]	4.4×10^{13} pkm	2015
POM[34]	1.2×10^6 tonnes	2016
PP[35]	5.3×10^7 tonnes	2014

S1.6. Emission factors for supporting activities

Table S8 presents the emission factors and references of the upstream supporting activities used in the study.

Table S8: References of emission factors used in the study. The allocation methods used by the sources are indicated between parentheses where applicable.

Parameter	Source	Value
Electricity	Renewable[36]	0.024 kg CO_2eq/kWh
	Natural gas[36]	0.49 kg CO_2eq/kWh
	Coal[30]	0.80 kg CO_2eq/kWh
Steam	Geothermal[36]	0.0017 kg CO_2eq/MJ
	Natural gas industrial boiler[37]	0.052 kg CO_2eq/MJ
Heat	Electrical heater (renewable electricity)[36]	0.024 kg CO_2eq/kWh
	Natural gas industrial furnace[38]	0.25 kg CO_2eq/kWh
	Combined heat and power[22]	0.35 kg CO_2eq/kWh (Exergy)
Hydrogen	Electrolysis (low carbon electricity)[39]	0.98 kg CO_2eq/kg H_2
	Steam methane reforming[40]	11 kg CO_2eq/kg H_2
	Coal gasification[41]	24 kg CO_2eq/kg H_2
CO_2 Capture Process	DAC[42] powered by low carbon energy	0.034 kg CO_2eq/kg CO_2
	Natural gas power plant[43]	0.18 kg CO_2eq/kg CO_2 (Substitution)
	DAC[42] powered by NG-based energy	0.39 kg CO_2eq/kg CO_2

S2. Sensitivity analysis to test assumptions (CO_2-based polymers)

Regarding the sensitivity analysis to investigate the influence of assumptions on the results (Fig. 5 in the main text), additional comments follow.

The CO_2 source appears at the bottom of the graph, indicating a weaker influence than the electricity source. The use of CO_2 from air and low carbon energy can reduce the net GHG emissions by 4.5% for PP, compared to the base case. The use of CO_2 from air and natural gas energy can increase the net emissions by 7.3% compared to the base case.

For the end-of-life treatment, for each 1 kg of virgin polymer produced, a total of 1.48 kg of useful polymer is produced (1 kg of virgin polymer + 0.48 kg of recycled polymer),[21] which translates to 0.67 kg of virgin polymer per kg of useful material. Therefore, less virgin CO_2-based polymer is needed, and the additional energy required to recycle is included. In the incineration process, heat and electricity are co-produced, which receive credits in the system expansion via substitution method to handle multiple products. The end-of-life treatment results in lower influence on the results, with the direct incineration presenting more pronounced effects to increase the net GHG emissions compared to the base case (18% for PP) than the recycling plus incineration reduces the net GHG emissions compared to the base case (4.4% for PP). Thus, avoiding the production of virgin CO_2-based polymers by recycling may result in slightly lower GHG emissions than the base case and direct incineration, as indicated by Lazarevic et al.,[44] who suggested that recycling tends to result in lower impacts to global warming compared to incineration.

The assumption for the energy demand in secondary units (methanol synthesis for PP) presented the lowest influence on the net GHG emissions of the parameters tested in this sensitivity analysis, with ±7.0% compared to the base case.

Figure S2 presents the breakeven analysis for CO_2-based polymers according to varying electricity emissions intensity.
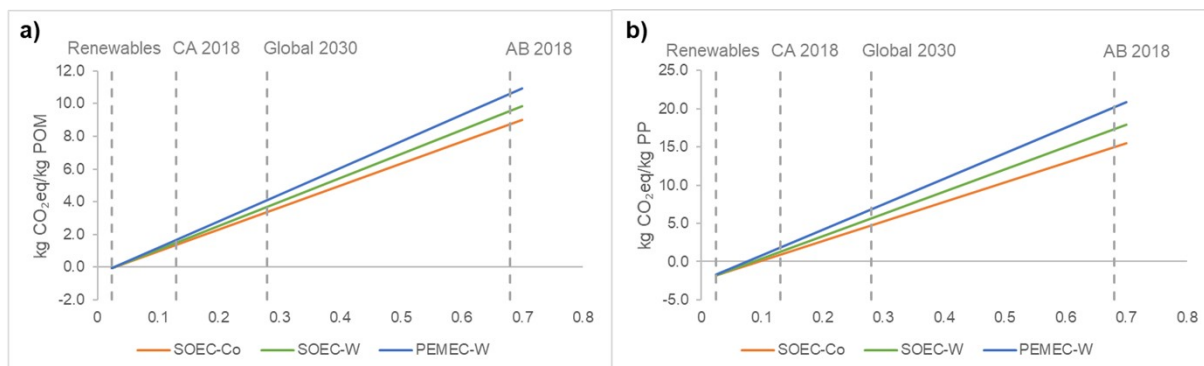

Figure S2: Net GHG emissions of CO_2-based (a) POM and (b) PP depending on the electricity emissions intensity. The vertical dashed lines represent different electricity emissions intensities, varying from an average renewable electricity to the average electricity grid in the Alberta province, in Canada.

For POM, electricity emissions intensities above 0.029 kg CO_2eq/kWh will likely result in positive net GHG emissions per kg of CO_2-based POM produced and used. For PP, the breakeven electricity emissions intensity is 0.094, 0.086, and 0.075 kg CO_2eq/kWh for SOEC-Co, SOEC-W, and PEMEC-W, respectively. The electricity emissions intensity of the projected global average for 2030 (0.28 kg CO_2eq/kWh,[45] labeled as "Global 2030"), the average of electricity emissions intensity in Alberta province, in Canada for 2018 (0.68 kg CO_2eq/kWh,[46] labeled as "AB 2018"), and the national average of electricity emissions intensity in Canada for 2018 (0.14 kg CO_2eq/kWh,[46] labeled as "CA 2018") are not low enough to result in neutral net GHG emissions for CO_2-based POM and PP. However, the electricity emissions intensity in the

provinces of Quebec (0.002 kg CO_2eq/kWh)[46] and Ontario (0.03 kg CO_2eq/kWh)[46] in Canada, for example, the electricity emissions intensities are low enough to be GHG-emission-reducing for production and use of CO_2-based polymers.

Figure S3 presents the sensitivity analysis for the market penetration assumption to estimate the global emissions reduction potential (SOEC-W). In the base case, a 50% market penetration was assumed for all cases, and this percentage was varied to 25% and 75%. CO_2-based chemicals applied to transportation may be as interesting as power generation if a 75% market penetration for transportation is achieved and if the market penetration for power generation is 25%, from a global perspective. CO_2-based chemicals applied to polymer production are likely not to result in higher global emissions reduction than transportation and power generation, not even with 75% market penetration.
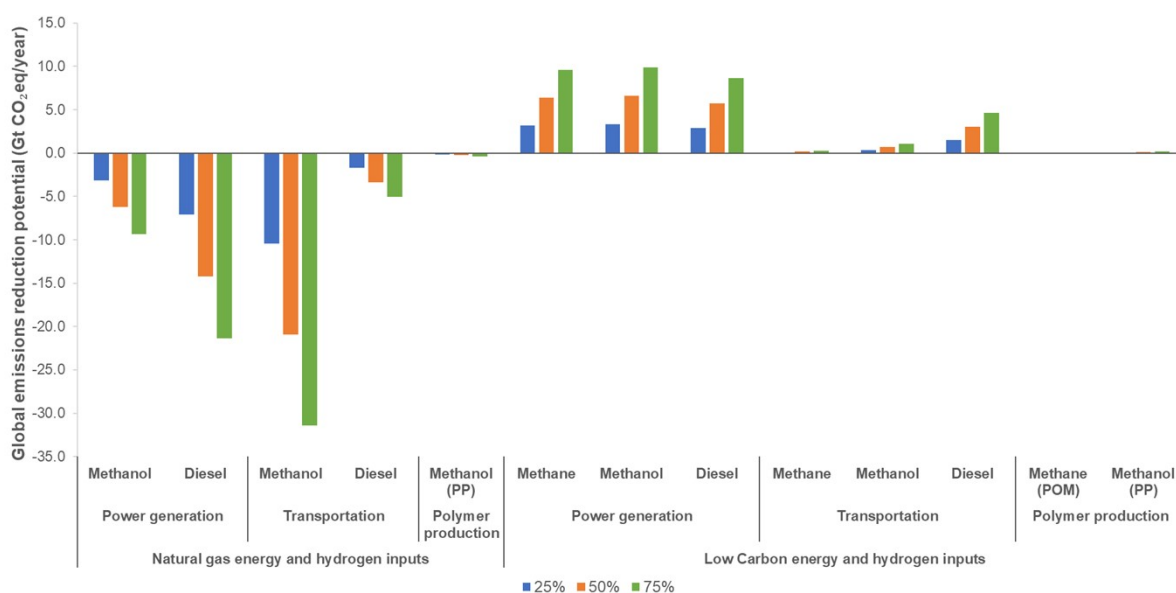

Figure S3: Sensitivity analysis for the global emissions reduction potential depending on the market penetration in each application of CO_2-based chemicals.

S3. Sensitivity analysis for influential parameters (CO_2-based diesel production)

The sensitivity analysis was performed on diesel production by SOEC water electrolysis. Figure S4 presents a simplified diagram of the process and Table S9 the parameters and ranges tested in the sensitivity analysis.

The reference studies from Okeke and Mani,[6] Okeke et al.,[5] and Zhang et al.[18] were used to develop the diesel production process via water electrolysis and Fischer-Tropsch. Data provided in the supporting Information of Van der Giesen et al.[7] was also used. A process simulator was not employed, so the integration between the two pieces was done manually, and the following assumptions were made:

- The heat produced in the F-T and upgrade is sufficient to meet demand from the reverse water gas shift reactor and to generate steam for electrolysis.
- The unconverted gas from F-T is used to generate electricity that partly offsets the imported electricity.

The main product analyzed is diesel. The co-products are oxygen, steam, wax, gasoline, and LPG.
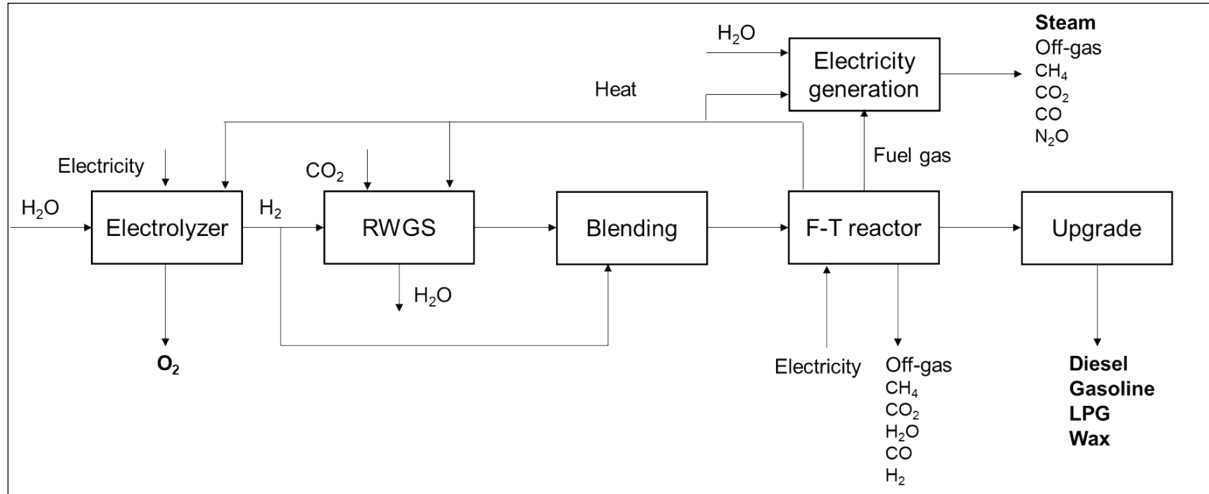

Figure S4: Diagram of diesel production from water electrolysis and F-T process.

Table S9: Factors included in the sensitivity analysis for LCA and economic performance for diesel production.

Factor	Analysis	Lower range	Higher range	Base case
Electricity source[30,36,47]	LCA and Economic	Low-carbon	Coal-based	Natural gas-based
SOEC degradation[48]	LCA and Economic	0.1%	2%	0.5%
Allocation method	LCA	Mass allocation	No allocation	System expansion via substitution
Stack cost[18,49]	Economic	1251 $/kW	2348 $/kW	2000 $
Energy demand (H_2 production)[50,51]	LCA and Economic	28 kWh/kg H_2	50 kWh/kg H_2	46 kWh/kg H_2
Electrochemical process[7,10]	LCA and Economic	Co-electrolysis (SOEC-Co)	Water electrolysis (PEM-W)	Water electrolysis (SOEC-W)
CO_2 source[43,52,53]	LCA and Economic	DAC + low carbon energy	DAC +NG energy	Natural gas power plant
F-T conversion[6]	LCA and Economic	64%	96%	80%
Lifetime of stacks[18,54]	LCA and Economic	12 kh	100 kh	48 kh

S3.1. LCA
S3.1.1.   Infrastructure

The infrastructure construction datasets for electrolyzer, reverse water gas shift reactor, F-T unit, and electricity generation unit, as well as catalyst production, were based on Van der Giesen et al.[7] This integrated analysis involves TEA, which includes costs of equipment. Thus, the boundary for this LCA analysis was expanded to include the manufacturing of equipment.

As a note, the manufacturing phase or construction of equipment and production plants may be excluded from the boundary as the impacts from the construction phase are "amortized" over their lifetime, often resulting in only small contributions to the life cycle impacts of products. Conversely, the operations phase is often responsible for most impacts. Processes that have high energy demands (including non-spontaneous processes such as electrolysis) are highly affected by the GHG emissions of the source of energy, which can vary from 0.02 kg CO_2eq/kWh[36] for renewables to 0.49 kg CO_2eq/kWh[29] for natural gas, almost a 20-fold difference.

S3.1.2.   Operations

This sub-section provides information about the operations phase. The output is 1.1×10^3 kg of diesel/hr, and this value was used to calculate emissions on a per kg of diesel basis.

The amount of hydrogen necessary and the equipment properties were obtained from Van der Giesen et al.[7] The electricity demand is 46 kWh/kg H_2, and 11 kg of H_2O is needed per kg of H_2 produced. The number of stacks was calculated based on hydrogen production per stack provided by Zhang et al.[18] For the reverse water gas shift unit, for each kg of carbon monoxide, 1.6 kg of CO_2 and 0.07 kg of H_2 are needed. The catalyst is composed of CuO (57%), ZnO (31%), and Al_2O_3 (11%), while the water adsorbent is considered a zeolite powder. Regarding heat, it is considered that the integration with the Fischer-Tropsch unit provides enough energy to run the unit.[7]

For the Fischer-Tropsch unit, Okeke et al.[5] and Okeke and Mani[6] described the same system and were used as the reference. The system sizing and hydrocarbon production were based on Okeke and Mani,[6] and the intermediate streams were calculated based on Okeke et al.[5] The H_2:CO ratio in the syngas is 2.2. The process is a low temperature (200 °C and 30 bar with cobalt catalyst) reaction in a slurry phase reactor. The conversion is 80% in this unit. For upgrading and separation, light fractions were collected as LPG. Hydrocracking (380 °C and 50 bar with platinum catalyst) processed the wax fraction, and hydrotreating (distillate and naphtha, with cobalt catalyst), diesel and olefins, to yield the final products.

In total, the emissions per hour are 1.2×10^4 kg CO_2eq/hr, or 8.5×10^3 kg CO_2eq/hr considering the CO_2 uptake (with full credits for use). Van der Giesen et al.[7] evaluated a similar system. However, the authors lumped all the fuels produced in the F-T unit, the electrolyzer considered was alkaline, the oxygen was not considered as a co-product,

and the emissions from the F-T unit were not considered. Nevertheless, the magnitude of impacts was similar. In the base case, the impacts are 0.11 kg CO_2eq/MJ considering the energy of co-products, while Van der Giesen et al.[7] obtained between 0.01 and 0.22 kg CO_2eq/MJ (without the combustion phase). In the low carbon, the diesel impacts are -0.02 kg CO_2eq/MJ, and Van der Giesen et al.[7] obtained -0.04 kg CO_2eq/MJ. The results were also compared to Liu et al.,[17] who reported between 12 and 29 g CO_2eq/MJ of F-T fuel, depending on the DAC system for CO_2 capture from air. By applying the corresponding assumptions to our system, we obtained 24 g CO_2eq/MJ, which we considered reasonable.

S3.2. Economics

The equipment costs were scaled using the appropriate scale factors, and the prices were inflated using either CE or Marshall and Swift indexes, depending on the reference.

S3.2.1. Capital investment

The capital investment of the Fischer-Tropsch piece was obtained from Okeke and Mani.[6] For the electrolysis portion, the purchase cost was first estimated based on base costs from the literature and scaled to the size of the system in this work by applying the equation below:[18]

$$C_{BM} = C_{p,ref}^0 \left(\frac{A}{A_{ref}^0}\right)^m$$

(S1)

where C_{BM} is the bare module cost of the equipment, which is the cost of equipment accounting for the different size or capacity as compared to a reference cost. The factors A_{ref}^0 and $C_{p,ref}^0$ are the capacity and cost from literature, A is the capacity of the equipment that we wish to estimate the cost, and m is the cost exponent.

The method described by Towler and Sinnott[55] was used to estimate the costs of equipment from the electrolysis piece. The equation below estimates the purchase cost of common plant equipment:

$$C_{BM} = a + bS^n$$

(S2)

where a, b and n are constants specific for each equipment, S is the size parameter. Towler and Sinnott[55] provide a table with parameters for common plant equipment, relative to U.S Gulf Coast in January 2006 (CE index of 478.6).

When the cost is relative to the past, the cost can be adjusted to the present by applying cost indexes via the equation below:

$$C^t = C^0 \left(\frac{I_{index}}{I_{ref,index}} \right)$$
(S3)

where C^t is the cost in the time considered for the project, C^0 is the cost found in the literature relative to past years, I_{index} is the cost index for the time of the project, and $I_{ref,index}$ is the cost index for the time considered in the literature record. In this work, two indexes are used: Marshall and Swift for the water gas shift reactor[18] and CE index for equipment such as compressors, flash drums, heat exchangers.

To estimate the total capital investment, the approach described by Okeke and Mani[6] was applied. The total sum of equipment cost (TEC) was the basis for the remaining calculations, as the equations below show:

$$BOP = 0.12 \, TEC$$
(S4)

$$TDEC = TEC + BOP$$
(S5)

$$IEC = 0.89 \, TDEC$$
(S6)

$$TPC = TDEC + IEC$$
(S7)

$$Contingency \, fee = 0.204 \, TPC$$
(S8)

$$FCI = TPC + Contingency \, fee$$
(S9)

$$WC = 0.1 \, FCI$$
(S10)

$$Land = 0.08 \, TEC$$
(S11)

$$TCI = FCI + WC + Land$$
(S12)

where BOP is the balance of plant, TDEC is the total direct equipment cost, IEC is the indirect equipment cost, TPC is the total plant cost, FCI is the fixed capital investment, WC is the working capital, and TCI the total capital investment.

Table S10 presents the parameters for the electrolysis piece, the stacks and reverse water gas shift unit.[18]

Table S10: Parameters for electrolyzer and reverse gas shift reactor cost calculation.

Equipment	$C_{p.ref}^{0}$ (M$)	A_{ref}^{0}	unit	Base year	m
Single stack of the electrolyzer[18]	2×10^{-3}	-	-	-	-
Reverse water gas shift reactor[56]	12.2	8819	kmol $(CO+H_2)$/hr	2002	0.65

The stack price is relative to a lifetime of approximately 48,000 hours.[18] Schmidt et al.[54] mention a wide range of lifetime, and the values are relative to expert opinions of future lifetimes of SOEC by 2020. Two ranges were mentioned: 6 to 15 kh (academic expert) and 50 to 100kh (industry expert). A study commissioned by the European Union and published in 2019[49] reported as state of the art, 8-20 kh of SOEC stacks lifetime. It was estimated that with the highest degradation rate, a lifetime of 12 kh would be a

reasonable assumption. For the higher end, the 100 kh was based on the reported values in the literature; therefore, a range of 20 to 100 kh of lifetime was selected for the sensitivity analysis. Zhang et al.[18] mention the Marshall and Swift index for 2017 as 1593.7. The index for the base year of 2002 is 1096.4.

The CAPEX for the F-T, upgrade, and electricity generation units was calculated based on the breakdown of results provided by Okeke and Mani,[6] resulting in 49 MM$. The total CAPEX of the plant is 147 MM$. The corresponding annual capital costs[57] considers the interest rate to annualize the capital costs (see Table S13). The levelized annual capital charge rate (LACCR), 11.75%, is based on a 10% interest rate and 20 years plant lifetime. The annual capital costs result in 17 MM$.

S3.2.2.   Operational cost

The operational cost has variable and fixed components, as the equation below[55] describes:

$$Cash\ cost\ of\ production = Costs_{variable\ +\ fixed} - Byproduct\ revenues \qquad \text{(S13)}$$

The operational cost includes raw materials (reagents, catalysts), electricity, and labor. Co-product revenues are related to selling oxygen, steam, wax, gasoline, and LPG. It is assumed that these co-products can be commercialized.

In terms of labor, Okeke and Mani[6] provides a breakdown of positions in each production area. Thus, in the F-T/upgrading and separation/administrative areas, the numbers provided by Okeke and Mani[6] were used. To estimate the number of operators in the electrolysis and RGWS areas, the procedure based on Turton et al.[58] and described by Zhang et al.[18] was used.

$$N_{OS} = \left(6.29 + 31.7P^2 + 0.23N_{eq}\right)^{0.5} \qquad \text{(S14)}$$

where N_{OS} is the number of operators per shift, P is the number of processes involving particulate solids (e.g., transportation and distribution), and N_{eq} is the number of equipment (e.g., compressor and heat exchangers).

The operators needed in all shifts were calculated by:

$$N_{TO} = 4.5\ N_{OS} \qquad \text{(S15)}$$

where N_{TO} is the total number of operators in all shifts.

Table S11 summarizes the positions and salaries.

Table S11: Positions and salaries of employees considered in the diesel production.

Position	Quantity	Salary ($/yr)	Total ($/yr)
Plant manager	1	147,000	147,000
Plant engineer	2	70,000	140,000

Maintenance supervisor	1	57,000	57,000
Maintenance tech	6	40,000	240,000
Lab manager	1	56,000	56,000
Lab technician	1	40,000	40,000
Shift supervisor	2	48,000	96,000
Shift operators	24	48,000	1,152,000
Clerks and secretaries	3	36,000	108,000
Total			2.0×10^6

Other fixed operating costs (OFOC) was estimated according to Table S12.[6] The Total fixed operating costs is calculated by:

$$Total\ fixed\ operating\ costs = Total\ salaries + OFOC \qquad (S16)$$

Table S12: Other fixed operating costs considered in the diesel production.

Cost	Calculation expression
Labor burden	0.9 Total salaries
Maintenance	0.03 FCI
Property insurance	0.007 FCI

Table S13 lists the main assumptions in the techno-economic assessment.

Table S13: Assumptions made in the economic assessment of base case diesel production.

Economic data	value	unit
Plant lifetime[6]	20	year
Interest rate[59]	10	%year
Annual operating hours[6]	8000	hours/year
Electricity price (natural gas)[60]	0.07	$/kWh
Gasoline price[61]	2.4	$/gal
LPG[62]	2.8	$/gal
Oxygen price[16]	177	$/t
Catalyst (Cobalt)[6]	35	$/kg
Catalyst (Platinum)[6]	56	$/kg
Catalyst (WGSR)[18]	18	$/kg
Catalyst lifetime (RWGS)[7,18]	4	year
Carbon dioxide[63]	60	$/t
Process water price[6]	0.2	$/t

The metric used in the sensitivity analysis is the net production cost (NPC),[64] which includes the ACC (annual capital costs), operational costs, and revenue from co-products, normalized by the annual production of diesel.

$$NPC(\$/kg\ diesel) = \frac{ACC + OPEX}{annual\ diesel\ production} \qquad (S17)$$

The calculated cost of diesel production is \$2.5/kg or \$7.7/gal. Rafati et al.[57] reported a cost of ~1.8 \$/kg (5.6 \$/gal) of FT liquids from biomass gasification, and Dimitriou et al.[65] obtained ~\$1.7 - \$3.4/kg (\$5.3 - \$10.6/gal) of FT fuels from H_2 (water electrolysis) and CO_2 (sewage sludge). Thus, the cost obtained in this study was considered reasonable. It is worth noting that the goal of this study is not to evaluate the economic feasibility of diesel but investigate potential trade-offs between economic and environmental aspects.

Regarding the lower and higher inputs, for the LCA and TEA sensitivity, the emission factors are listed in Table S9. The remaining economic factors are listed in Table S14.

Table S14: Remaining economic factors associated with the parameters tested in the economics sensitivity analysis.

Parameter	Lower input	Higher input
Source of electricity (\$/kWh)[60]	0.09 (Renewable)	0.08 (Coal)
Source of CO_2 (\$/tCO_2)[52,63]	200 (DAC)	-

The renewable electricity cost is an average of low-carbon sources, which includes lower cost hydropower and higher cost nuclear electricity.[60] The coal electricity has become unpopular recently, which in face of the cheaper natural gas-based electricity, results in increasing costs.[60]

S3.3. Additional comments on results of sensitivity

Regarding the sensitivity analysis for CO_2-based diesel production in the LCA and TEA study (Fig. 6 in the main text), additional conclusions to the presented in the main text can be drawn. The energy demand for H_2 production in the base case (i.e., via SOEC-W) was 46 kWh per kg H_2, with lower values found in the literature (28 kWh/kg H_2),[50] and consequently, lower GHG emissions. However, higher demand was also found (50 kWh/kg H_2),[51] resulting in higher GHG emissions. The production costs follow the same trend according to the electricity consumption, which reduces the price for lower energy demand, and increases for higher energy demand.

For the economic analysis, the stack cost was placed in the same row as allocation, as these factors only related to one side of the analysis. In this case, intuitively, lower stack costs lead to lower production costs, and the opposite is true for higher stack costs.

The electrolysis pathway also influences net GHG emissions. Co-electrolysis resulted in lower emissions due to lower hydrogen and electricity demand, while PEM resulted in higher emissions, compared to SOEC water electrolysis. Unlike the other factors, both alternative processes resulted in lower production costs. This is because PEM is a commercially established and cheaper technology compared to SOEC; thus, capital investment is lower enough to compensate for the higher electricity consumption.

For co-electrolysis, the operational costs, such as electricity, are lower compared to SOEC water electrolysis.

Regarding CO_2 capture, the source was varied to DAC powered by natural gas energy (higher value) and DAC powered by low carbon energy (lower value). We assume that energy for capturing CO_2 from the flue gas in a natural gas power plant (base case) is provided by natural gas in the plant. For DAC in the lower value, we assumed low carbon electricity is used to capture CO_2 from air, resulting in lower emissions, while DAC in the higher value is powered by natural gas-based energy, resulting in higher emissions. Results indicate that this parameter is of interest, demonstrating that factors external to the electrochemical process may affect the net GHG emissions.

For diesel production, the processes following the electrolyzer may also affect environmental and economic performance. In this work, we evaluated the conversion to diesel in the F-T unit. Lower conversion rates lead to higher emissions and higher production costs because more energy and input materials are needed to produce the same amount of diesel. Therefore, it is important to consider the entire production plant when evaluating potential applications for electrolyzers.

S3.4. Additional results and interpretation - Avoided emissions and global reduction potential

The second set of metrics, as mentioned in Section 2.2 of the main text, focuses on evaluating the carbon conversion technologies consistently, regardless of the application or the product generated, and identifying potential benefits of the carbon conversion technologies compared to incumbent processes. The second set of metrics includes kg CO_2eq emitted per kg CO_2eq converted, avoided emissions, and global emissions reduction potential.

The kg CO_2eq emitted/kg CO_2 converted metric may be used to evaluate CCT alternatives in terms of the amount of the CO_2 captured that is converted. It sets a plain field among CCTs used for different applications, allowing comparison across technologies. The avoided emissions metric compares the net emissions of incumbent and CCT processes. Incumbent technologies refer to technologies currently used on a commercial scale, e.g., natural gas extraction and refining for methane. The avoided emissions may be calculated by Equation S18, and it is intended to quantify the benefits (if any) of CCTs in terms of GHG emissions, compared to incumbent production processes.

$$Avoided\ emissions = Incumbent\ net\ CO_2eq\ emissions - CCT\ net\ CO_2eq\ emissions \quad \text{(S18)}$$

Negative results mean that CCT options (in this case, electrolysis) result in more GHG emissions than the incumbent technology. Alternatively, a positive value indicates that electrolysis may result in lower GHG emissions, avoiding emissions from incumbent technologies. Consider that the conventional PP production process results in 1.9 kg CO_2eq/kg PP. If a CCT alternative results in 1.0 kg CO_2eq/kg PP, there is likely a climate benefit in choosing the CCT, which translates to 0.9 kg CO_2eq/kg PP avoided (1.9 – 1.0 kg CO_2eq/kg PP). On the other hand, if the CCT results in 2.0 kg CO_2eq/kg PP, there is

likely no climate benefit in choosing the CCT, which translates to -0.1 kg CO_2eq/kg PP of (not) avoided emissions metric (1.9 – 2.0 kg CO_2eq/kg PP).

The last metric envisions the potential of a given CCT to reduce emissions, in mass of CO_2eq, globally per year. The global reduction potential is calculated according to Equation S19. For this case study, the market sizes as of 2014 or more recent found in the literature are considered, and 50% market penetration is assumed in the base case and is varied in the sensitivity analysis. Future work will employ more sophisticated models for this metric, but the purpose of this work is to estimate the potential that each case presents to reduce the global GHG emissions. The results presented in this study are high-level estimates.

$$Global\ emissions\ reduction\ potential = Avoided\ emissions\ x\ Market\ size\ x\ 50\%\ market\ penetration$$
(S19)

Consider the PP production via CCT again, with 0.90 kg CO_2eq/kg PP of avoided emissions, as commented above. The PP market size as of 2014 is 5.3×10^7 tonnes per year[32]. In this case, considering a 50% market penetration, the global emissions reduction potential would be 24 Gt per year (0.9 kg CO_2eq/kg PP x 5.3×10^{10} kg/year x 0.5).

In terms of the results of kg CO_2eq/kg CO_2 converted metric shown in Figure S5, the different applications evaluated may be presented together using this metric since it considers only the CO_2 emitted and converted, regardless of the application. It also allows better visualization of the potential for a technology to convert more CO_2 than it emits. All fuels in the base case resulted in positive numbers, meaning that the cases considered will likely result in more CO_2eq emissions than the amount each case can convert. In the low carbon scenario, methane and methanol applied to polymer production resulted in negative values (-0.56 kg CO_2eq/kg CO_2 converted for POM, and -0.75 kg CO_2eq/kg CO_2 converted for PP, SOEC-W), indicating that these cases may be better than the absence of CCT use.
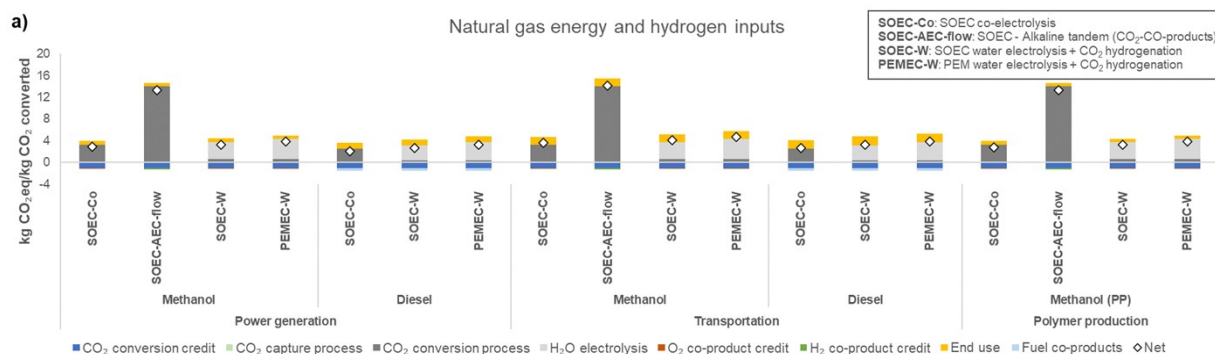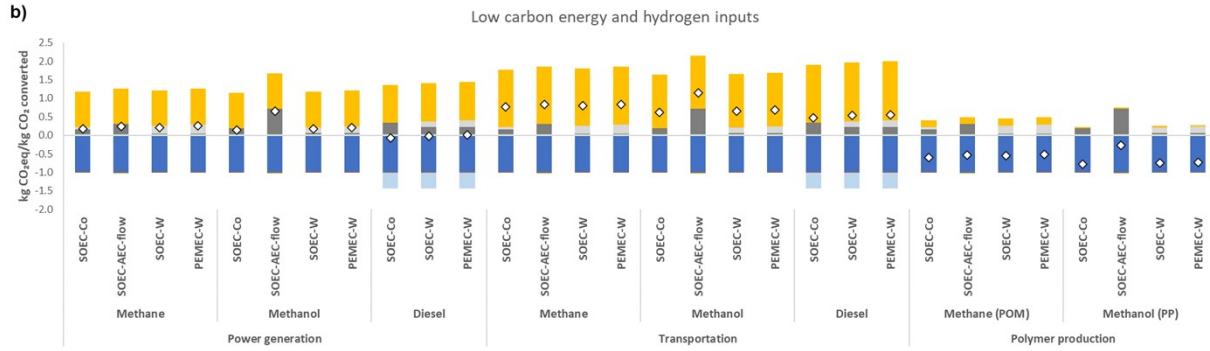
Figure S5: Life cycle GHG emissions in kg CO_2eq/kg CO_2 converted in power generation, transportation and polymer production of SOEC co-electrolysis, SOEC (CO_2 to CO) followed by alkaline flow cell (CO to products), SOEC water electrolysis, and PEM water electrolysis, (a) in natural gas energy and hydrogen inputs and (b) low carbon energy and hydrogen inputs.

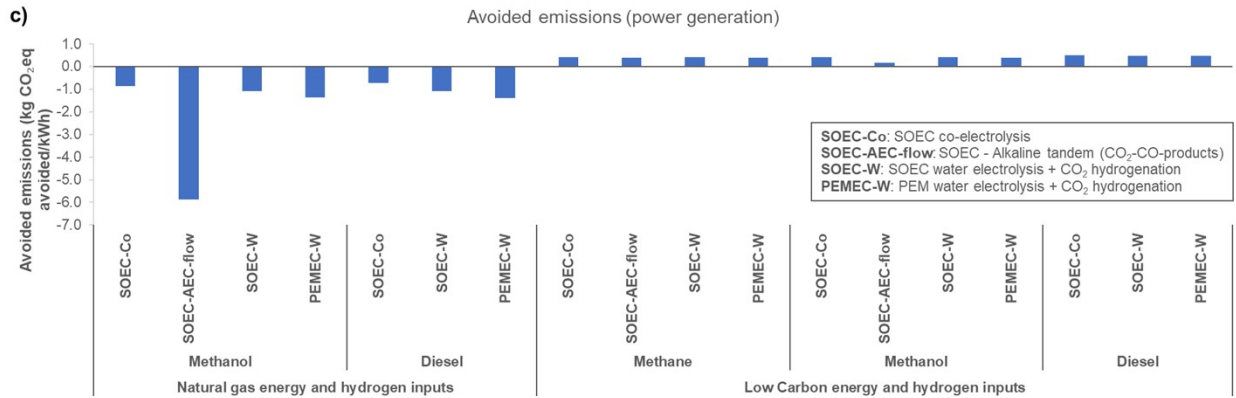Figure S6 presents the avoided emissions for the base case and low carbon scenarios.
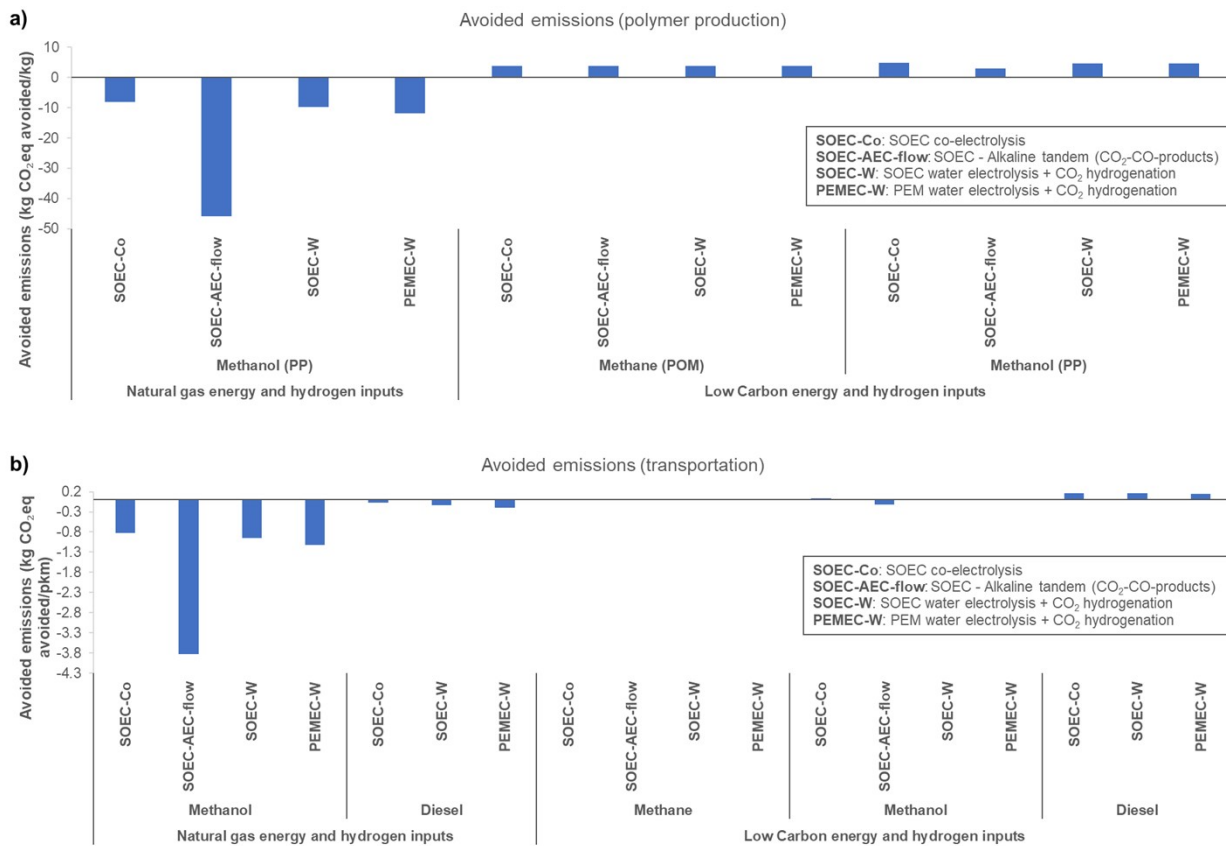
Figure S6: Avoided emissions of fuel production by electrolysis applied to (a) polymer production, (b) transportation and (c) power generation, for natural gas energy and low carbon energy and hydrogen inputs.

This metric is dependent on the application considered, so each application is represented by one figure. In this case, the CO_2-based production is compared to the incumbent process according to Equation S18, with negative numbers indicating that the CO_2-based alternative emits more GHG than incumbent processes and positive values indicating that the CO_2-based options may result in lower emissions. CO_2-based options with natural gas-derived sources of electricity and CO_2 (the base case) result in more GHG emissions than the incumbent options for all applications. However, using low carbon sources, electrochemical solutions potentially avoid emissions compared to incumbent technologies. Therefore, power generation, transportation, and polymer production from CO_2-based fuels are beneficial only in a low carbon scenario. This result suggests that jurisdictions with a low carbon grid are the most promising for electrochemical processes. Another possibility is to pair the electrochemical process with a low carbon source of electricity, such as nuclear or solar plants. Studies analyzing electrochemical processes designed to be coupled to a low carbon source of energy may be found in the literature.[66–68]

The avoided emissions metric does not capture the potential that each application presents on a global basis. Thus, the global emissions reduction potential metric incorporates the market size in the analysis to provide a sense of scale. Figure S7 presents the global emissions reduction potential of all cases considered according to Equation S19. Unlike the avoided emissions metric, different applications may be represented in the same figure because the y-axis does not depend on the application.

From Figure S7, only in a low carbon scenario, CO_2-based alternatives reduce the impacts on the climate.

Polymer production appeared as a promising application in a low carbon scenario, according to Fig. 2 (in the main text) and Figure S6. However, considering the smaller market size compared to power generation and transportation, this end use results in a lower potential to reduce emissions globally. Therefore, even though looking individually at each application, polymer production seems to be the best choice for achieving

emissions reductions, when considering incumbent production processes and market sizes, power generation and transportation may result in greater emission reductions. Methanol from CO_2 electrolysis applied to transportation is the exception, due to the low efficiency in this application and to the high energy requirement in the electrolysis/separation process.
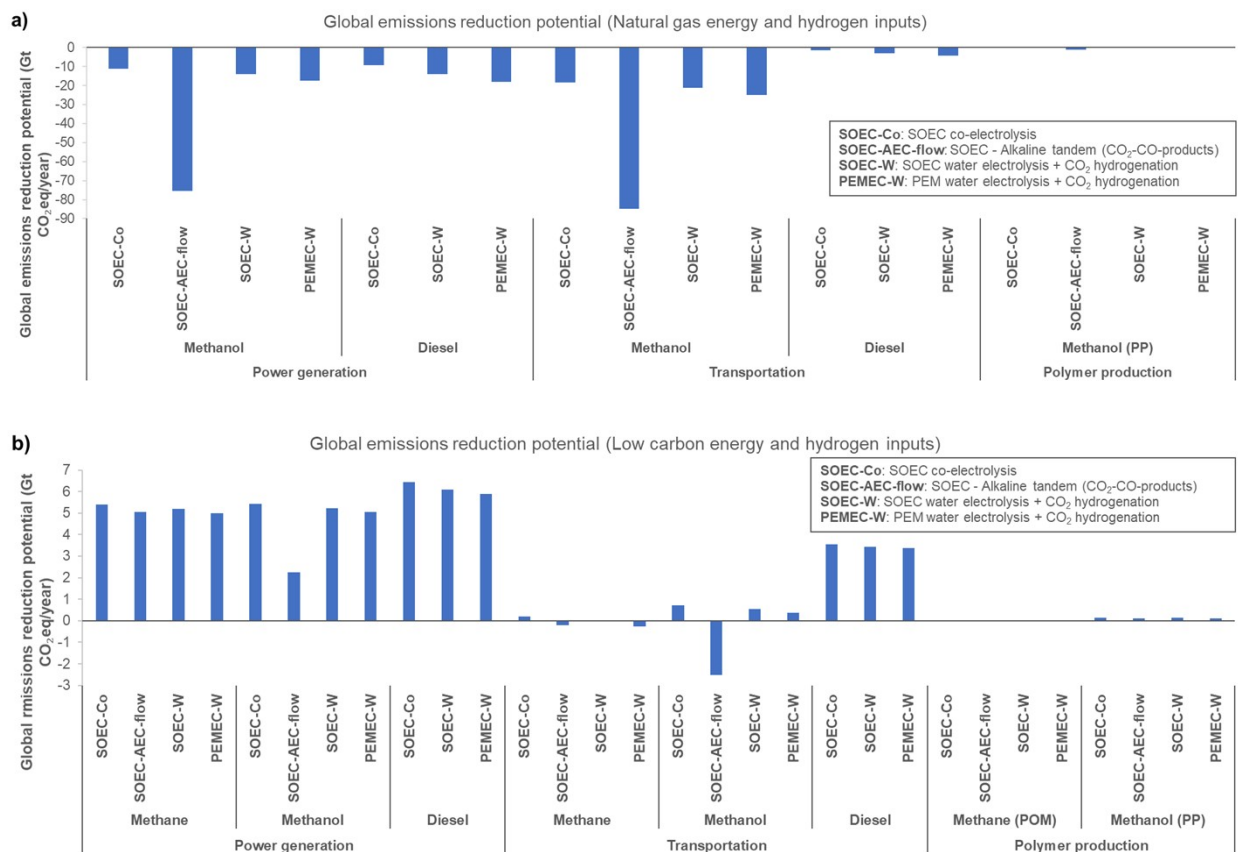

Figure S7: Global GHG emissions reduction potential per year related to power generation, transportation, and polymer production, in Gigatons of CO_2eq/year, of CO_2-based fuels in (a) base case (natural gas sources) and (b) low carbon (renewable sources) scenarios.

S4.   Allocation methods

In LCA studies, a boundary determines the system that will be analyzed. The impacts are studied relative to the main function of the system, which can be the main product generated or a service. In the sensitivity analysis, the intended function is the production of diesel. However, in many systems, additional functions are also outputs; in the diesel case, the additional outputs are the other products (oxygen, steam, gasoline, LPG, wax). Hauschild[69] provides a good discussion about multifunctional systems in chapter 8, subitem 8.5.

The ISO standard[70,71] recommends that whenever possible, a sub-division should be done to account for the multiple functions of the system. With this method, the entire system is broken into smaller pieces, resulting in the identification of which sub-processes generate each function (or product). Therefore, the impacts of each function (or product) are related to those specific generating sub-processes. However, this method is not applicable to the diesel case, given that multiple products are generated from only one sub-process (F-T unit, for instance, which produces diesel, gasoline, LPG, and wax).

The next recommended method is system expansion, in which the boundaries of the system are expanded to include alternative processes that generate the additional functions (or products). The alternative processes may be conventional (or incumbent) processes of production. In the oxygen case, for instance, the alternative process is cryogenic air separation.[72,73] In this method, the functional unit includes the output of the alternative production processes; in diesel case, the functional unit would be x kg of diesel and y kg of O_2. However, the interest of the sensitivity is only diesel. Thus, system expansion via substitution was considered.

With substitution, the studied main system is considered to avoid the alternative production process of the co-products, oxygen in this case. Therefore, the electrolysis/F-T process produces oxygen as a co-product, and this oxygen avoids the same amount of oxygen produced by the cryogenic air separation method. In the calculation of impacts, this is done by subtracting the impacts of alternative oxygen production from the total impacts of the system under study. Due to the subtraction, negative emissions attributed to the main function (or product) may be obtained. As Müller et al.[42] pointed out, the negative result does not imply capture of greenhouse gases, or necessarily a net-negative process. The negative impact signifies that the system under study (diesel production from electrolysis/F-T) considering all the co-products, results in lower emissions than the impacts of incumbent production of the main product (diesel in this case) in addition to the incumbent production processes of the co-products.

Table S15 lists the incumbent processes of the co-products in the system.

Table S15: Incumbent production process of the co-products generated in the electrolysis/F-T diesel production.

Co-product	Alternative production process
Oxygen	Cryogenic air separation[31]
Steam	Steam from natural gas boiler[30]
Gasoline	Gasoline Blendstock from Crude Oil[30]
LPG	Liquid Petroleum Gas from Natural Gas[30]
Wax	Paraffin production (Proxy)[22]

The last option to account for the multifunctionality is allocation. In this method, the impacts of the system are partitioned among the products following a certain relationship. The preferred relationship is physical properties, such as mass or energy content of products. Other used relationships are of economic nature (e.g., market prices).

Figure S8 presents the impacts of diesel production, employing different methods to account for the co-products. The highest impact, as expected, is obtained if no method is used and all the burden is attributed to diesel. This option would result in an unfair load of impacts on diesel, and the other co-products would be considered "burden-free". The second column in Figure S8 is relative to the method chosen in the study, in which the co-products presented in Table S15 are avoided by the electrolysis/F-T production of diesel. The last three columns present the impacts of diesel production, applying allocation, and different relationships. For this study, the three options were not considered adequate for the system under study. If the energy content of products is considered, O_2 would not have an allocation factor assigned to it, resulting in a burden-free co-product. If the economic value is applied, the impact fluctuates according to the market, which is not ideal. Figure S9 illustrates the magnitude of variability considering different market prices of O_2 found in the literature.[49,74]

In any alternative case the order of allocation method changes, i.e., the market price of oxygen does not make economic allocation result in lower emissions than mass allocation or higher emissions than energy allocation. The economic allocation would only become the extreme case (i.e., result in lower allocated emissions to diesel) if the price of oxygen reaches approximately $1700/t, which does not seem likely, but it highlights the volatility involved in economic allocation. Lastly, if the mass is considered to calculate the allocation factors, the impacts would be attributed in most part to O_2, which is the product with the highest mass output; however, it is not the main product of interest (or the reason the system would be built).
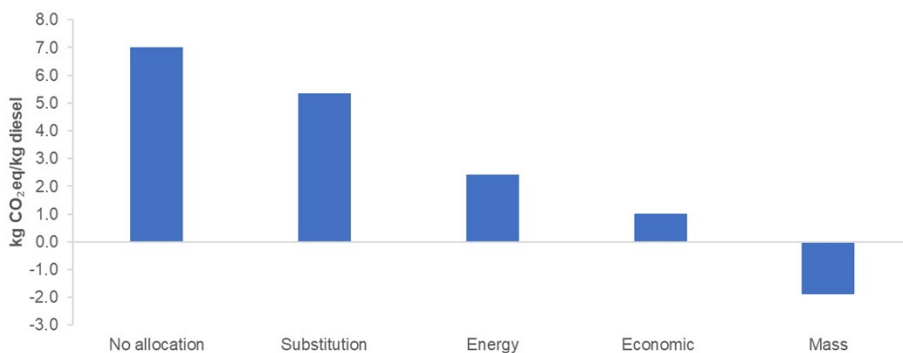

Figure S8: Influence of methods to account for multifunctionality of the diesel production system.
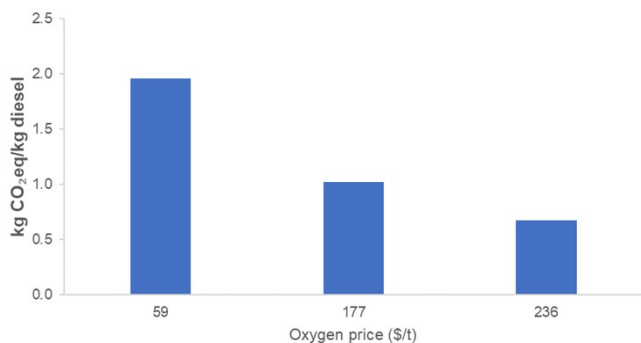
Figure S9: Impact of prices of oxygen on the impacts of diesel production considering economic allocation.

S5. Considerations about other environmental impacts

Past studies have estimated other environmental impacts of CO_2-conversion processes and compared them to incumbent or biomass-based counterparts. However, the majority do not provide a breakdown of the impacts, only a total number. While sufficient to characterize the process as it was proposed, it does not help draw conclusions that can be applied to other configurations. Additionally, the interpretation of results tends to stop at the contributor without further explanations (e.g., water provision is an important driver, but the reason is not explored). Therefore, in this section, we review some of the main findings in past studies and further explain the results, which could support decision-making during R&D or deployment stages.

As with GHG emissions, the source of electricity is the key driver for most other environmental impacts, with water electrolysis for H_2 production as a main contributor.[75] In general, CO_2-based alternatives result in higher impacts than the incumbents when powered by fossil sources. This is the case for acidification and eutrophication for CO_2-based ethylene production,[75,76] for example, because the upstream electricity generation from sources such as natural gas emits acid gases (leading to higher acidification indicators) or nitrogen oxides (leading to higher eutrophication indicators), both mostly from natural gas production[22]. When the source of electricity is changed to wind, for example, the impacts of CO_2-based products become lower than the fossil incumbent. Some studies consider different sources of electricity for H_2 production. Meunier et al.[77] and Yang et al.[78] consider water electrolysis for H_2 generation powered exclusively by wind electricity, whereas CO_2 capture and conversion are powered by European and China grid mixes, respectively. If it is possible to generate H_2 from non-fossil energy sources (e.g., by selecting a specific H_2 supplier), it may help reduce the total impacts because, as Keller et al.[75] noted, electricity for water electrolysis is the main driver of acidification and eutrophication.

Interestingly, when comparing CO_2-based ethylene with a biomass-based counterpart, acidification and eutrophication tend to be higher for the biomass case, even

considering natural gas-based electricity powering the CO_2-based alternative. The agricultural phase is the main responsible for the higher impacts. In maize cultivation for syngas production,[75] for example, ammonia from the mineral fertilizers released into the air during the agricultural phase is the main driver of the acidification impact. For eutrophication, nitrates released into the water during the agricultural phase are the most important contributor, with ammonia in second[22]. Therefore, if a biomass component is needed, characterizing the feedstock appears to be the most relevant piece considering local impacts such as acidification and eutrophication.

As mentioned, water electrolysis for H_2 generation is one of the main contributors to impacts. In addition to the impacts from the electricity input directly to electrolysis, Biernacki et al.[79] noted that the provision and treatment of water for CO_2-based methanol production in Germany may also lead to increased impacts on photochemical oxidation. However, this also depends on the electricity used to exploit and treat water. Comparing the same water treatment located in Europe (powered by European grid mix) with water treatment located in Quebec/Canada (powered by mostly hydroelectricity in Quebec grid), the contribution of electricity source changes substantially, leading to 70% less photochemical oxidant formation impacts in Quebec case.[22]

Still related to water, but in terms of consumption, the water electrolysis alone is responsible for over 70% of the consumption in Yang et al.[78] study for CO_2-based methanol production in China. The result agrees with Meunier et al.[77] study on CO_2-based methanol production in Germany. Therefore, the water demand of this unit may also help define the location or conditions for deployment (in addition to the electricity source as mentioned above).

It is estimated that for each kg of H_2, 18 to 24 kg of water is needed prior to treatment[51]. In the pathways considered in this study, methane would require 9 – 13 kg water/kg methane, methanol would require 3 – 5 kg water/kg methanol, and diesel would require 7 – 10 kg water/kg diesel (SOEC-W, just for H_2 production). Considering diesel production on the scale proposed by Okeke et al.[6] (3 million gallons of diesel/year) and the minimum consumption of 5 L of water/person in a day, the water used only for H_2 production in a diesel plant could support between 35,000 – 50,000 in a year. The acceptance depends on the region and the respective availability of water. IRENA[51] also mentions that if water is assumed to be sourced from the ocean and desalinized, this aspect is not as important from a water consumption point of view.

References

1   S. Rönsch, J. Schneider, S. Matthischke, M. Schlüter, M. Götz, J. Lefebvre, P. Prabhakaran and S. Bajohr, *Fuel*, 2016, **166**, 276–296.
2   W. Hoppe, N. Thonemann and S. Bringezu, *J. Ind. Ecol.*, 2018, **22**, 327–340.
3   B. Müller, K. Müller, D. Teichmann and W. Arlt, *Chemie Ing. Tech.*, 2011, **83**, 2002–2013.

4   L. K. Rihko-Struckmann, A. Peschel, R. Hanke-Rauschenbach and K. Sundmacher, *Ind. Eng. Chem. Res.*, 2010, **49**, 11073–11078.

5   I. J. Okeke, K. Sahoo, N. Kaliyan and S. Mani, *J. Clean. Prod.*, 2020, **249**, 119358.

6   I. J. Okeke and S. Mani, *Biofuels, Bioprod. Biorefining*, 2017, **11**, 472–487.

7   C. Van Der Giesen, R. Kleijn and G. J. Kramer, *Environ. Sci. Technol.*, 2014, **48**, 7111–7121.

8   S. Kibria Nabil, S. McCoy and M. G. Kibria, *Green Chem.*, 2021, **23**, 867–880.

9   A. Paturska, M. Repele and G. Bazbauers, *Energy Procedia*, 2015, **72**, 71–78.

10   Q. Fu, C. Mabilat, M. Zahid, A. Brisse and L. Gautier, *Energy Environ. Sci.*, 2010, **3**, 1382–1397.

11   E. Giglio, A. Lanzini, M. Santarelli and P. Leone, *J. Energy Storage*, 2015, **1**, 22–37.

12   R. G. Grim, Z. Huang, M. T. Guarnieri, J. R. Ferrell, L. Tao and J. A. Schaidle, *Energy Environ. Sci.*, 2020, **13**, 472–494.

13   J. Sisler, S. Khan, A. H. Ip, M. W. Schreiber, S. A. Jaffer, E. R. Bobicki, C.-T. Dinh and E. H. Sargent, *ACS Energy Lett.*, 2021, **6**, 997–1002.

14   C. M. Gabardo, C. P. O'Brien, J. P. Edwards, C. McCallum, Y. Xu, C.-T. Dinh, J. Li, E. H. Sargent and D. Sinton, *Joule*, 2019, **3**, 2777–2791.

15   A. Quindimil, U. De-La-Torre, B. Pereda-Ayo, A. Davó-Quiñonero, E. Bailón-García, D. Lozano-Castelló, J. A. González-Marcos, A. Bueno-López and J. R. González-Velasco, *Catal. Today*, 2020, **356**, 419–432.

16   W. Haije and H. Geerlings, *Environ. Sci. Technol.*, 2011, **45**, 8609–8610.

17   C. M. Liu, N. K. Sandhu, S. T. McCoy and J. A. Bergerson, *Sustain. Energy Fuels*, 2020, **4**, 3129–3142.

18   H. Zhang, L. Wang, M. Pérez-Fortes, J. Van herle, F. Maréchal and U. Desideri, *Appl. Energy*, 2020, **258**, 114071.

19   PlasticsEurope, Polyoxymethylene (POM) Eco-profiles and Environmental Product Declarations of the European Plastics Manufacturers, https://www.plasticseurope.org/en/resources/eco-profiles, (accessed 4 November 2020).

20   W. Keim, Ed., *Kunststoffe*, Wiley, 2006.

21   S. Turnau, C. S. Mignot, C. Mostert and S. Bringezu, *Green Chem.*, 2020, **22**, 8423–8443.

22   G. Wernet, C. Bauer, B. Steubing, J. Reinhard, E. Moreno-Ruiz and B. Weidema, *Int. J. Life Cycle Assess.*, 2016, **21**, 1218–1230.

23   C. A. Trudewind, A. Schreiber and D. Haumann, *J. Clean. Prod.*, 2014, **70**, 38–49.

24   A. Simons, *Int. J. Life Cycle Assess.*, 2016, **21**, 1299–1313.

25   F. Brunner, Natural gas production, https://www.ecoinvent.org/support/ecoinvent-forum/topic.html?&tid=448, (accessed 4 August 2020).

26   S. Schori and R. Frischknecht, *Life Cycle Inventory for Natural Gas Supply*, Uster, Switzerland, 2012.

27   Y. Bicer and F. Khalid, *Int. J. Hydrogen Energy*, 2020, **45**, 3670–3685.

28   C. Strazza, A. Del Borghi, P. Costamagna, M. Gallo, E. Brignole and P. Girdinio, *Energy Convers. Manag.*, 2015, **100**, 64–77.

29   D. Ravikumar, G. Keoleian and S. Miller, *Appl. Energy*, 2020, **279**, 115770.

30   Argonne National Laboratory, *GREET Model*, 2021.

31   P. Markewitz, J. Marx, A. Schreiber and P. Zapp, *Energy Procedia*, 2013, **37**, 2864–

2876.

32   IEA, Atlas of Energy - Electricity, http://energyatlas.iea.org/#!/tellmap/-1118783123, (accessed 4 November 2020).

33   J. Pagenkopf, B. van den Adel, Ö. Deniz and S. Schmid, in *Achieving the Paris Climate Agreement Goals: Global and Regional 100% Renewable Energy Scenarios with Non-energy GHG Pathways for +1.5C and +2C*, ed. S. Teske, Springer International Publishing, Cham, 2019, pp. 131–159.

34   J. Andrzejewski, B. Gapiński, A. Islam and M. Szostak, *Materials (Basel).*, 2020, **13**, 3496.

35   M2 Presswire, Synthetic and Bio-Based Polypropylene Market Demand Is Expected To Reach 87.35 Million Tons, Growing at a CAGR Of 5.2% from 2015 to 2022: Grand View Research, Inc., https://link.gale.com/apps/doc/A458544797/ITOF?u=ucalgary&sid=ITOF&xid=426 923dd, (accessed 4 November 2020).

36   Intergovernmental Panel on Climate Change, in *Climate Change 2014 Mitigation of Climate Change*, Cambridge University Press, Cambridge, 2015, pp. 1329–1356.

37   EPA, External Combustion Sources - Natural Gas Combustion, https://www3.epa.gov/ttn/chief/old/ap42/ch01/s04/final/c01s04_oct1996.pdf, (accessed 10 December 2020).

38   ISCC, GHG Emission Requirements V1.1, https://www.iscc-system.org/wp-content/uploads/2018/01/ISCC-PLUS-205-01-GHG-Emission-Requirements-1.1.pdf, (accessed 10 December 2020).

39   D. R. Simbeck and E. Chang, *Hydrogen Supply: Cost Estimate for Hydrogen Pathways – Scoping Analysis*, Mountain View, California, 2002.

40   P. L. Spath and M. K. Mann, *Life Cycle Assessment of Hydrogen Production via Natural Gas Steam Reforming*, 2001.

41   A. Mehmeti, A. Angelis-Dimakis, G. Arampatzis, S. McPhail and S. Ulgiati, *Environments*, 2018, **5**, 24.

42   L. J. Müller, A. Kätelhön, S. Bringezu, S. McCoy, S. Suh, R. Edwards, V. Sick, S. Kaiser, R. Cuéllar-Franca, A. El Khamlichi, J. H. Lee, N. von der Assen and A. Bardow, *Energy Environ. Sci.*, 2020, **13**, 2979–2992.

43   Helmeth Consortium, *Deliverable 5.2: Final LCA Report HELMETH concept system*, 2017.

44   D. Lazarevic, E. Aoustin, N. Buclet and N. Brandt, *Resour. Conserv. Recycl.*, 2010, **55**, 246–259.

45   S. Deutz and A. Bardow, *Nat. Energy*, 2021, **6**, 203–213.

46   Environment and Climate Change Canada, *National inventory report 1990 - 2018: Greenhouse gas sources and sinks in Canada*, Gatineau, QC, 2020.

47   EIA, Short-Term Energy Outlook - Forecast highlights, https://www.eia.gov/outlooks/steo/report/electricity.php, (accessed 10 December 2020).

48   Q. Fang, L. Blum and N. H. Menzler, *J. Electrochem. Soc.*, 2015, **162**, F907–F912.

49   A. Zauner, H. Böhm, D. C. Rosenfeld and R. Tichler, *Innovative large-scale energy storage technologies and Power-to-Gas concepts after optimization. D7.7 Analysis on future technology options and on techno-economic optimization*, 2019.

50   IEA, Hydrogen Production & Distribution, https://www.iea.org/reports/iea-energy-

technology-essentials-hydrogen-production-distribution, (accessed 10 December 2020).

51 IRENA, *Green Hydrogen Cost Reduction: Scaling up Electrolysers to Meet the 1.5 C Climate Goal*, 2020.

52 D. W. Keith, G. Holmes, D. St. Angelo and K. Heidel, *Joule*, 2018, **2**, 1573–1594.

53 IPCC, *IPCC Special Report on Carbon Dioxide Capture and Storage. Prepared by Working Group III of the Intergovernmental Panel on Climate Change [Metz, B., O. Davidson, H. C. de Coninck, M. Loos, and L. A. Meyer (eds.)].*, 2005.

54 O. Schmidt, A. Gambhir, I. Staffell, A. Hawkes, J. Nelson and S. Few, *Int. J. Hydrogen Energy*, 2017, **42**, 30470–30492.

55 G. Towler and R. Sinnott, *Chemical Engineering Design: Principles, Practice and Economics of Plant and Process Design*, Elsevier Science, 2007.

56 C. N. Hamelinck, A. P. C. Faaij, H. den Uil and H. Boerrigter, *Energy*, 2004, **29**, 1743–1771.

57 M. Rafati, L. Wang, D. C. Dayton, K. Schimmel, V. Kabadi and A. Shahbazi, *Energy Convers. Manag.*, 2017, **133**, 153–166.

58 R. Turton, R. C. Bailie, W. B. Whiting and J. A. Shaeiwitz, *Analysis, Synthesis and Design of Chemical Processes*, Pearson Education, 2002.

59 J. Q. Albarelli, S. Onorati, P. Caliandro, E. Peduzzi, M. A. A. Meireles, F. Marechal and A. V. Ensinas, *Energy*, 2017, **138**, 1281–1290.

60 P. Breeze, in *The Cost of Electricity*, ed. P. Breeze, Elsevier, 2021, pp. 117–136.

61 EIA, US gasoline prices increased in 2017, https://www.eia.gov/todayinenergy/detail.php?id=34392, (accessed 14 May 2021).

62 U.S. DOE, *Clean Cities Alternative Fuel Price Report*, 2018.

63 IEA, Levelised cost of CO_2 capture by sector and initial CO_2 concentration, 2019, https://www.iea.org/data-and-statistics/charts/levelised-cost-of-co2-capture-by-sector-and-initial-co2-concentration-2019, (accessed 21 November 2020).

64 F. G. Albrecht, D. H. König, N. Baucks and R.-U. Dietrich, *Fuel*, 2017, **194**, 511–526.

65 I. Dimitriou, P. García-Gutiérrez, R. H. Elder, R. M. Cuéllar-Franca, A. Azapagic and R. W. K. Allen, *Energy Environ. Sci.*, 2015, **8**, 1775–1789.

66 P. Collet, E. Flottes, A. Favre, L. Raynal, H. Pierre, S. Capela and C. Peregrina, *Appl. Energy*, 2017, **192**, 282–295.

67 S. Ghandehariun and A. Kumar, *Int. J. Hydrogen Energy*, 2016, **41**, 9696–9704.

68 Q. Cai, C. S. Adjiman and N. P. Brandon, *J. Power Sources*, 2014, **268**, 212–224.

69 M. Z. Hauschild, *Life Cycle Assessment*, Springer International Publishing, Cham, 2018.

70 The International Standards Organisation, *Environmental Management—Life Cycle Assessment—Requirements and Guidelines (ISO 14044)*, 2006.

71 The International Standards Organisation, *Environmental Management—Life Cycle Assessment—Principles and Framework (ISO 14040)*, 2006.

72 J. B. Dunn, F. Adom, N. Sather, J. Han and S. Snyder, *Life-cycle Analysis of Bioproducts and Their Conventional Counterparts in GREET ™*, 2015.

73 NETL and DOE, *Baseline Technical and Economic Assessment of a Commercial Scale Fischer-Tropsch Liquids Facility*, 2007.

74 D. Bellotti, M. DIerks, F. Moellenbruck, L. Magistri, K. Görner and G. Oeljeklaus,

E3S Web Conf., 2019, **113**, 1–7.

75   F. Keller, R. P. Lee and B. Meyer, *J. Clean. Prod.*, 2020, **250**, 119484.

76   H. H. Khoo, I. Halim and A. D. Handoko, *J. CO2 Util.*, 2020, **41**, 101229.

77   N. Meunier, R. Chauvy, S. Mouhoubi, D. Thomas and G. De Weireld, *Renew. Energy*, 2020, **146**, 1192–1203.

78   N. Yang, F. Kang, Z. Liu, X. Ge and Y. Zhou, *Int. J. Low-Carbon Technol.*, 2022, **17**, 550–562.

79   P. Biernacki, T. Röther, W. Paul, P. Werner and S. Steinigeweg, *J. Clean. Prod.*, 2018, **191**, 87–98.